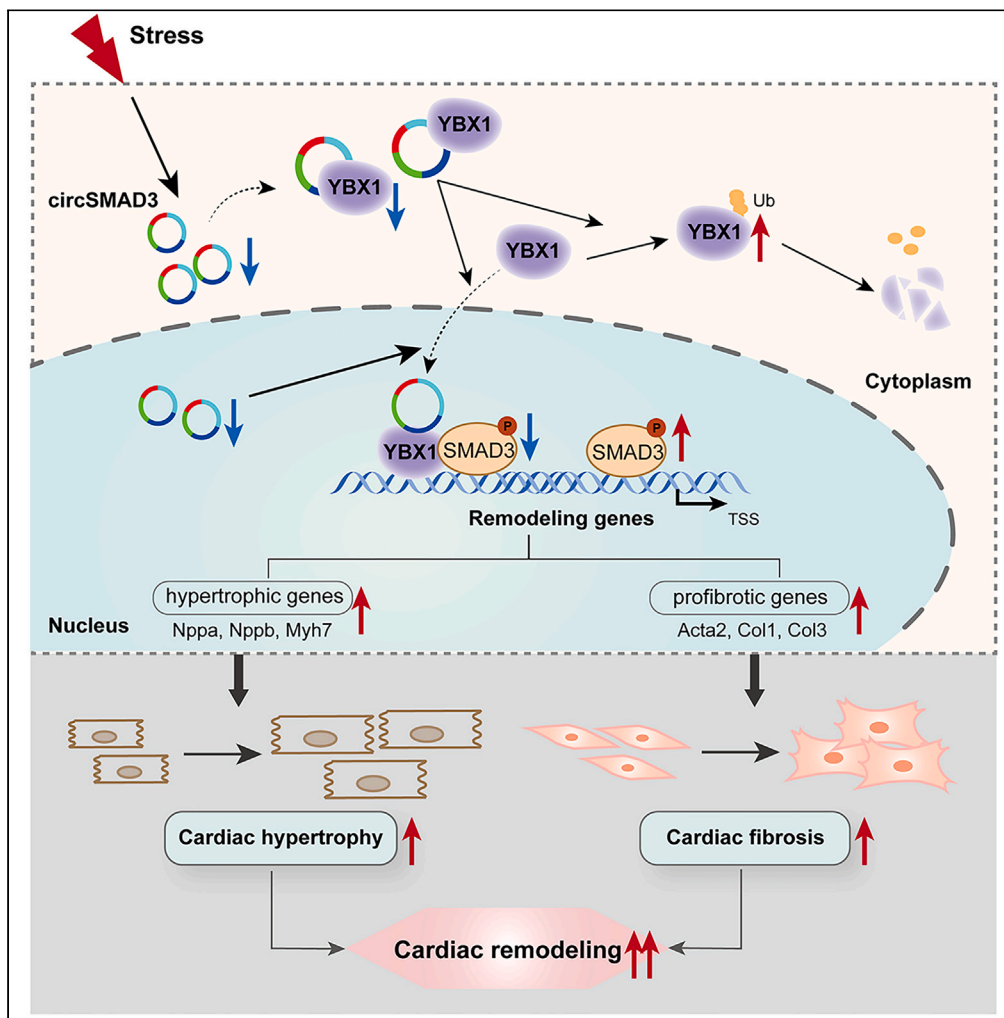


Article

# CircSMAD3 represses SMAD3 phosphorylation and ameliorates cardiac remodeling by recruiting YBX1



Shuai Mei, Xiaozhu Ma, Li Zhou, ..., Chen Chen, Jiangtao Yan, Hu Ding

jtyan@tjh.tjmu.edu.cn (J.Y.)  
dingo8369@163.com (H.D.)

Highlights

CircSMAD3 mitigates cardiomyocyte hypertrophy and deactivates cardiac fibroblast

CircSMAD3 interacts with YBX1 to disrupt the TGFβ/SMAD3 signaling pathway

Intervention targeting circSMAD3 is a potential treatment for heart failure

Mei et al., iScience 27, 110200  
July 19, 2024 © 2024 The Authors. Published by Elsevier Inc.  
<https://doi.org/10.1016/j.isci.2024.110200>



## Article

# CircSMAD3 represses SMAD3 phosphorylation and ameliorates cardiac remodeling by recruiting YBX1

Shuai Mei,<sup>1,2</sup> Xiaozhu Ma,<sup>1,2</sup> Li Zhou,<sup>1,2</sup> Qidamugai Wuyun,<sup>1,2</sup> Jing Wang,<sup>1,2</sup> Qianqian Xiao,<sup>1,2</sup> Man Wang,<sup>1,2</sup> Kaiyue Zhang,<sup>1,2</sup> Chen Chen,<sup>1,2</sup> Jiangtao Yan,<sup>1,2,\*</sup> and Hu Ding<sup>1,2,3,\*</sup>

**SUMMARY**

**Circular RNA (circRNA) has emerged as potential therapeutic targets for cardiovascular diseases. Given the central role of the TGF $\beta$  signaling pathway in cardiac remodeling and its potential as a therapeutic target, we hypothesized that a circRNA from this pathway could modulate cardiac remodeling and serve as a heart failure treatment. Therefore, we identified a circRNA, named circSMAD3, that was significantly reduced in murine heart failure models. Functionally, circSMAD3 mitigated cardiomyocyte hypertrophy and inhibited cardiac fibroblast activation *in vitro*. Mechanistically, circSMAD3 interacts with YBX1, stabilizing it and facilitating its binding to SMAD3 in the nucleus, disrupting the TGF $\beta$ /SMAD3 signaling pathway, and ultimately restoring cardiac remodeling. This study highlights circSMAD3 as a promising therapeutic target for heart failure treatment.**

**INTRODUCTION**

Heart failure is a major threat to human health and a substantial burden on society.<sup>1,2</sup> Despite many effective pharmacological therapies, no medicine exists to solve the residual risk of heart failure by repairing heart damage.<sup>3,4</sup> The transforming growth factor  $\beta$  (TGF $\beta$ ) signaling pathway is critical for modulating cardiac remodeling and heart failure.<sup>5,6</sup> Numerous studies have been conducted to identify critical anti-fibrotic targets, including antibodies or inhibitors, focusing on TGF $\beta$ 1 for heart failure treatment; unfortunately, less progress has been made because of the side effects caused by TGF $\beta$ 1's multiple functions.<sup>6,7</sup> Therefore, considering the clinical need, we hypothesized that targeting the downstream effector of TGF $\beta$  could be a vital therapeutic approach to mitigate the side effects induced by upstream molecules.

Circular RNAs (circRNAs), a type of non-coding RNA, have a covalently closed loop structure with no 5' caps and 3' tails, which originate from pre-RNA back-splicing events.<sup>8,9</sup> circRNAs can act as microRNA sponges,<sup>10</sup> bind to proteins,<sup>11</sup> modulate genetic transcription,<sup>12</sup> and translate proteins.<sup>13</sup> Given their special structure, they are more stable than linear RNAs in response to external stimulation, suggesting that they are excellent therapeutic targets for heart failure. However, the role of circRNAs in the molecular pathogenesis of heart failure remains unclear.

Considering the key implications of the TGF $\beta$  signaling pathway in fibrosis and cardiac hypertrophy and its promising attractive target for cardiac remodeling therapy, we hypothesized that a circRNA derived from this pathway may modulate cardiac remodeling and be a target for heart failure. Consequently, we aimed to identify the key circRNAs implicated in cardiac remodeling and elucidate their functions.

**RESULTS****Identification of circSMAD3 as a regulator involved in cardiac remodeling**

The canonical TGF $\beta$  signaling pathway is a classic pathway that is critical for cardiac fibrosis and hypertrophy in heart failure. Therefore, to identify functional circRNAs as key epigenetic regulators, we initially focused on 89 circRNAs originating from the TGF $\beta$  signaling pathway (Figures 1A, S1A, and S1B). Notably, one of the functional circRNAs, hsa\_circ\_0003973, named circSMAD3 because of its parent gene, was identified in cardiomyocytes by Sanger sequencing and was significantly downregulated in transverse aortic constriction (TAC) and myocardial infarction (MI) (Figures 1B and 1D). Furthermore, circSMAD3 was downregulated in cardiomyocytes and cardiac fibroblasts isolated from the heart of the TAC model after 8 weeks (Figure 1C). Immunofluorescence further verified this result in cardiomyocytes and cardiac

<sup>1</sup>Division of Cardiology, Departments of Internal Medicine, Tongji Hospital, Tongji Medical College, Huazhong University of Science and Technology, Wuhan 430030, People's Republic of China

<sup>2</sup>Hubei Key Laboratory of Genetics and Molecular Mechanisms of Cardiological Disorders, Wuhan 430030, China

<sup>3</sup>Lead contact

\*Correspondence: [jtyan@tjh.tjmu.edu.cn](mailto:jtyan@tjh.tjmu.edu.cn) (J.Y.), [dingo8369@163.com](mailto:dingo8369@163.com) (H.D.)

<https://doi.org/10.1016/j.isci.2024.110200>



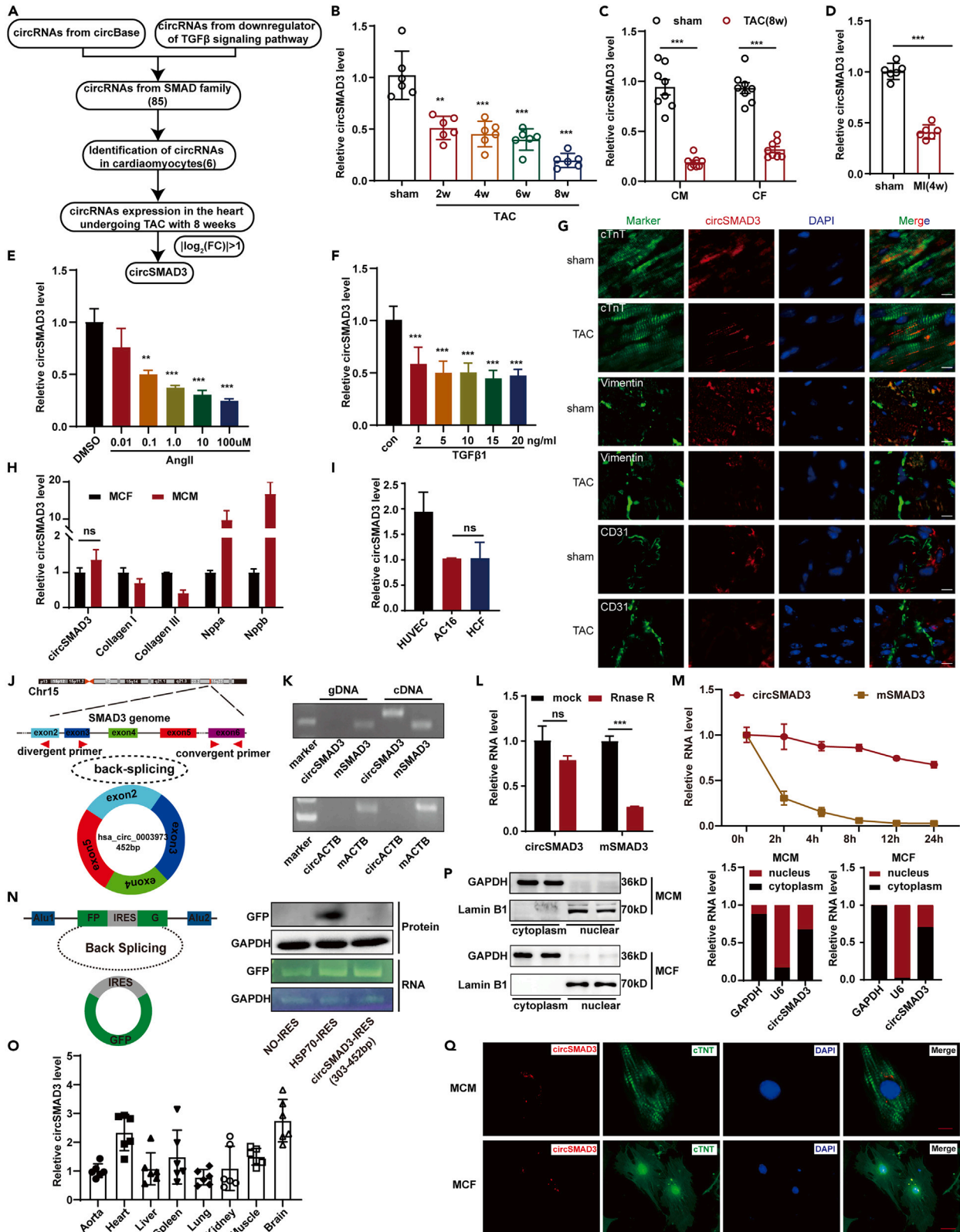


**Figure 1. Identification of circSMAD3 as a regulator of cardiac remodeling**

- (A) The schematic of the identification of circSMAD3 in SMAD family.
- (B) The expression of circSMAD3 in mouse heart with or without undergoing TAC. (n = 6 per group).
- (C) The expression of circSMAD3 in cardiomyocytes and cardiac fibroblasts separated from mouse heart with or without undergoing TAC. (n = 8 per group).
- (D) The expression of circSMAD3 in mouse heart with or without undergoing myocardial infarction (MI). (n = 6 per group).
- (E) The expression of circSMAD3 in cardiomyocyte in response to different concentration of angiotensin II. (n = 6 per group).
- (F) The expression of circSMAD3 in cardiomyocyte in response to different concentration of TGFβ1. (n = 6 per group).
- (G) The expression of circSMAD3 in mouse heart with or without undergoing TAC. TnT was the marker of cardiomyocyte. CD31 was the marker of endothelial cells and Vimentin was the marker of cardiac fibroblasts. Scale bar = 10 μm. (n = 5 per group).
- (H) The distribution of circSMAD3 in mouse primary cardiomyocytes and cardiac fibroblasts. (n = 6 per group).
- (I) The distribution of circSMAD3 in Human derived cardiomyocytes, cardiac fibroblasts and endotheliocyte. (n = 6 per group).
- (J) The schematic of circSMAD3 derived from SMAD3 gene.
- (K) Divergent primers amplified circSMAD3 in cDNA but not genomic DNA (gDNA). (n = 6 per group).
- (L) qPCR assays to detect circSMAD3, mSMAD3 with or without RNase R treatment. (n = 6 per group).
- (M) qPCR assays to detect circSMAD3, mSMAD3 with or without actinomycin D treatment in different times (0 h, 2 h, 4 h, 8 h, 12 h, 24 h). (n = 6 per group).
- (N) Schematic illustration (left) and application of the circRNA translation reporter system in 293T cells (right) using IRES-Hsp70 and circSMAD3 IRES plasmids.
- (O) The distribution of circSMAD3 in mouse tissues. (n = 6 per group).
- (P and Q) Cytoplasmic and nuclear RNA extraction assay (P) and RNA fluorescence *in situ* hybridization (FISH) (Q) showed that circSMAD3 was predominantly localized in cytoplasm, and some exist in nuclear. Scale bar = 10 μm. (n = 9 per group). *p* values correspond to two-tailed unpaired *t* tests for C, D, H, L, P and R; one-way ANOVA with Tukey's multiple comparisons test for B, E, F, M and O; data are presented in B–D and O as the mean ± SEM. Data are presented in E–I, L, M, and P as the mean ± SD of 3 independent experiments. \*\*\**p* < 0.001, \*\**p* < 0.01, \**p* < 0.05.

fibroblasts (Figures 1G and S1C). Consistent with the results in the two models, circSMAD3 was also decreased in primary cardiomyocytes (MCM) stimulated with angiotensin II (Ang II) and in cardiac fibroblasts (MCF) stimulated with TGFβ1, which are strong cytokines involved in cardiac remodeling (Figures 1E and 1F). The expression of circSMAD3 was similar in cardiomyocytes and cardiac fibroblasts (Figures 1H and 1I). These results demonstrate that circSMAD3 is a regulator that participates in cardiac remodeling.

Next, the properties of circSMAD3 were investigated. The length of circSMAD3 was 452 nt, originating from exons 2 to 5 of the SMAD family member 3 (*SMAD3*) gene (GeneBank: NM\_005902) (Figure 1J). Similar to the features of other circRNAs, endogenous circSMAD3 was more stable than linear RNA after RNase R digestion and actinomycin D treatment (Figures 1K–1M). circSMAD3 was also demonstrated to have no translation capability and was mainly expressed in the heart and brain in mouse tissues (Figures 1N and 1O). CircSMAD3 was primarily located in the cytoplasm of cardiomyocytes and cardiac fibroblasts (Figures 1P and 1Q).

Short interspersed elements (SINEs) in flanking introns and RNA binding proteins are critical for the generation of circRNAs, such as ALU element.<sup>14</sup> As expected, we analyzed the flanking intron sequences of circSMAD3 using the NCBI BLAST tool and confirmed that the presence of ALU1 and ALU2 elements promoted expression of circSMAD3 (Figures S2A–S2C). However, DExH-Box Helicase 9 (DHX9) is a DNA duplex helicase that inhibits the production of circRNA.<sup>15</sup> DHX9 CLIP-seq demonstrated binding peaks in the region of flanking intron sequences of circSMAD3, and the motif of DHX9 binding in RNA was also present in the two Alu elements (Figures S2A, S2D, and S2E). In cardiac fibroblasts and cardiomyocytes, the protein level of DHX9 was obviously promoted by TGFβ1 and AngII stimulation (Figures S2F–S2H). Therefore, we speculated that DHX9 might participate in the generation of circSMAD3. As expected, silencing of DHX9 promoted the expression of circSMAD3 (Figures S2I and S2J). Accordingly, an RNA immunoprecipitation assay demonstrated that DHX9 enriched SMAD3 precursor RNA (preSMAD3) rather than circSMAD3 and messenger SMAD3 RNA (mRNA) (Figure S2K). Furthermore, angiotensin II significantly promoted the enrichment of SMAD3 precursor RNA by DHX9 rather than circSMAD3 and SMAD3 messenger RNA (mSMAD3) (Figure S2L). These results demonstrated that the biogenesis of circSMAD3 was controlled via the ALU element as well as the RNA binding protein-DHX9.

**circSMAD3 repressed cardiac myofibroblast activation induced by TGFβ1 *in vitro***

Cardiac fibroblasts were infected with circSMAD3-overexpressed adenovirus or circSMAD3-shRNA adenovirus to explore the effects of circSMAD3 on cardiac fibrosis. Overexpression of circSMAD3 inhibited the conversion of fibroblasts into myofibroblasts induced by TGFβ1, as indicated by decreased *ACTA2*, *Collagen I*, and *Collagen III* expression (Figures 2A and 2C), weakened proliferation (Figures 2E, 2K and 2M), and migration capabilities (Figures 2G and 2I). Conversely, circSMAD3 knockdown promoted myofibroblast activation (Figures 2B–2N).

**circSMAD3 suppressed cardiomyocytes hypertrophy induced by AngII *in vitro***

To further illustrate the function of circSMAD3 in cardiac hypertrophy, cardiomyocytes (MCM and AC16) were successfully transfected with circSMAD3 overexpressing and knockdown adenovirus, which had no effect on its parent gene. circSMAD3 overexpression significantly reduced the expression of hypertrophic marker genes, including *NPPA*, *NPPB*, and *MYH7* (Figures 3A and 3C), and decreased cardiomyocyte size stimulated by Angiotensin II (Figures 3E–3G). Contrastingly, circSMAD3 silencing upregulated the expression of hypertrophy marker genes (Figures 3B and 3D) and increased the cell area (Figures 3H–3J).

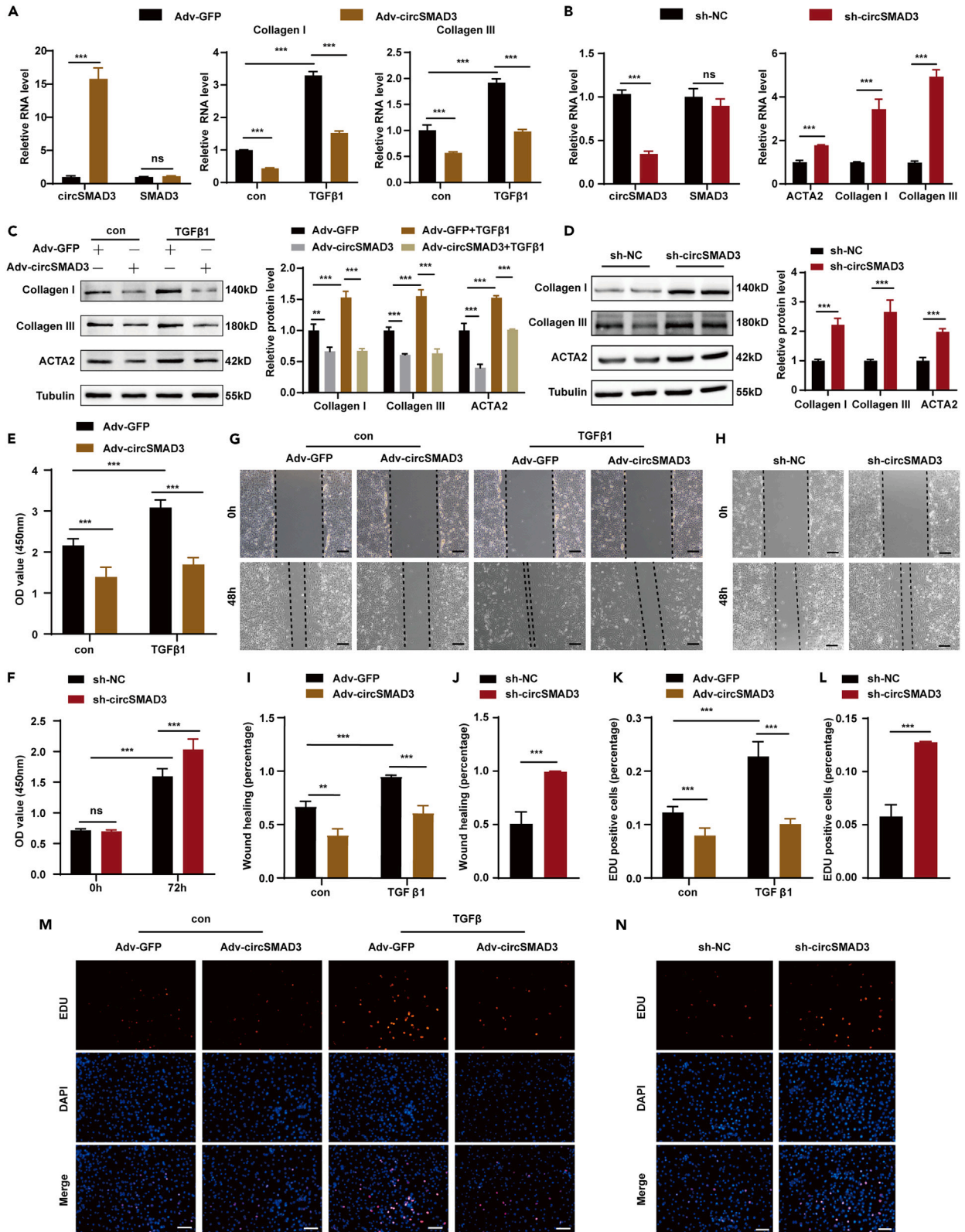


**Figure 2. circSMAD3 modulates cardiac fibroblasts activation *in vitro***

(A and B) qPCR assays to detect the overexpression (A) and silence (B) efficiency of circSMAD3 after being infected with circSMAD3 overexpressing or shRNA adenovirus and the expression of profibrotic genes in cardiac fibroblasts. (n = 9 per group).

(C and D) Western blot to detect profibrotic genes expression in protein levels after circSMAD3 overexpression (C) or silence (D) with or without TGFβ1 stimulation. (n = 6 per group).

(E and F) CCK8 assay to detect the proliferation of cardiac fibroblasts after circSMAD3 overexpression (E) or silence (F) with or without TGFβ1 stimulation. (n = 12 per group).

(G–J) Wound healing assay to evaluate the migration of cardiac fibroblasts after circSMAD3 overexpression (G&I) or silence (H&J) with or without TGFβ1 stimulation. Scale bar = 100 μm. (n = 6 per group).

(K–N) EDU assay to detect the proliferation of cardiac fibroblasts after circSMAD3 overexpression (K&M) or silence (L&N) with or without TGFβ1 stimulation. Scale bar = 50 μm. (n = 6 per group). p values correspond to two-tailed unpaired t tests for A, B, D, J and L; two-way ANOVA with Tukey's multiple comparisons test for A, C, E, F, I and K; data are presented as the mean ± SD of 3 independent experiments. \*\*\*p < 0.001, \*\*p < 0.01, \*p < 0.05.

**circSMAD3 deactivates TGFβ/SMAD3 signaling pathway by inhibiting SMAD3 phosphorylation**

Given the function of circSMAD3 in cardiac remodeling, we investigated the relationship between circSMAD3 and the TGFβ/SMAD3 signaling pathway. SMAD3 phosphorylation on serine 423 and serine 425 is activated when cardiac remodeling occurs. Therefore, we explored whether circSMAD3 affects SMAD3 phosphorylation in cardiac fibroblasts. As shown, circSMAD3 overexpression dramatically repressed SMAD3 phosphorylation induced by TGFβ1 and prominently decreased pSMAD3 in the nucleus (Figures 4A–4F). Furthermore, circSMAD3 silencing promoted the binding of SMAD3 to its target genes (Figure 4G). However, RNA pulldown and RIP assays demonstrated that circSMAD3 could not directly interact with SMAD3 and SMAD4 (Figure 4H). These results showed that circSMAD3 inhibited SMAD3 phosphorylation and indirectly participated in the TGFβ/SMAD3 signaling pathway.

**CircSMAD3 interacts with YBX1 to suppress its degradation by ubiquitination-protease pathway**

To further explore the molecular mechanisms of circSMAD3 modulating the phosphorylation modification of SMAD3, we identified critical proteins that interact with circSMAD3 from RNA pull-down products in primary cardiomyocytes and cardiac fibroblasts. To ensure the binding intensity of proteins to circSMAD3, we chose those proteins whose coverage rate exceeded 20% and existed in the two kinds of cells, and selected 14 proteins (Figure 5A). Among the selected products, Y-Box Binding Protein 1 (YBX1) has been reported to play a critical role in cardiac regeneration but serves as an antifibrotic factor in liver fibrosis. However, the function of YBX1 in cardiac remodeling has rarely been reported. Therefore, we selected YBX1 for further experiments. Further investigation using RNA pull-down and RNA immunoprecipitation (RIP) assays verified the direct binding of circSMAD3 to YBX1 in cardiomyocytes and cardiac fibroblasts (Figures 5B and 5C). Immunofluorescence staining showed that circSMAD3 colocalized with YBX1 in the cytoplasm of cardiomyocytes (Figure 5D). RNA-protein interaction tools-catRAPID<sup>16</sup> predicted that circSMAD3 mainly interacted directly with the C-terminus of YBX1 (Figure 5E), which was verified using an RNA pull-down assay with YBX1 truncated according to its domain (Figures 5F and 5G).

Further evaluation showed that the upregulation of circSMAD3 significantly promoted the expression of YBX1 at the protein level, whereas circSMAD3 downregulation regressed in primary cardiomyocytes and cardiac fibroblasts, while the mRNA expression of YBX1 remained unchanged (Figures 5H, 5I, S3A, and S3B). Furthermore, cytoplasmic nuclear separation and immunofluorescence assays in cardiomyocytes and cardiac fibroblasts revealed that circSMAD3 overexpression accelerated the transport of YBX1 to the nucleus (Figures 5J–5M, S3C, and S3D). Thus, circSMAD3 modulates YBX1 expression at the post-transcriptional level rather than at the transcriptional level. Considering that YBX1 is ubiquitinated and degraded by E3 ligase in various cancers,<sup>17,18</sup> we speculated that circSMAD3 maintains YBX1 stability by inhibiting the activation of the ubiquitin–proteasome pathway. Overexpression and silencing of circSMAD3 in neonatal mouse cardiomyocytes and cardiac fibroblasts decreased and increased ubiquitination levels, respectively (Figures S3E and S3F). Moreover, the decrease in YBX1 expression induced by circSMAD3 knockdown was attenuated by MG132, an inhibitor of ubiquitin–proteasome pathway (Figures 5N–5O). Subsequently, we constructed a YBX1 overexpression vector with a FLAG tag at the C-terminus, and a ubiquitin overexpression vector with an myc-tag. We observed that circSMAD3 significantly prevented ubiquitin enrichment in YBX1 and protected YBX1 from ubiquitination dependent on K33 (Figures 5P–5Q).

**circSMAD3 modulates cardiac fibrosis and hypertrophy dependent on YBX1**

Although the role of YBX1 in fibrosis has been investigated by many studies in several cancers, its role in cardiac hypertrophy and fibrosis remains poorly understood. We detected the expression of YBX1 in the heart failure model and observed that YBX1 decreased following the decline in Ang II and TGFβ1 and in a murine heart failure model induced by pressure overload (Figures S3G–S3J); however, the RNA levels did not change *in vitro* or *in vivo*. In cardiac fibroblasts, YBX1 overexpression inhibited the expression of profibrotic genes, including ACTA2, Collagen I, and Collagen III (Figures S4A and 4C), repressed cardiac fibroblast migration and proliferation induced by TGFβ1 (Figures S4E–S4M), YBX1 overexpression suppressed myofibroblast activation. Conversely, YBX1 silencing promoted myofibroblast activation (Figures S4B–S4N). In cardiomyocytes, YBX1 overexpression repressed the upregulation of hypertrophic marker genes and increase of cell area induced by Angiotensin II; Meanwhile, YBX1 silencing promoted (Figures S5A–S5H).

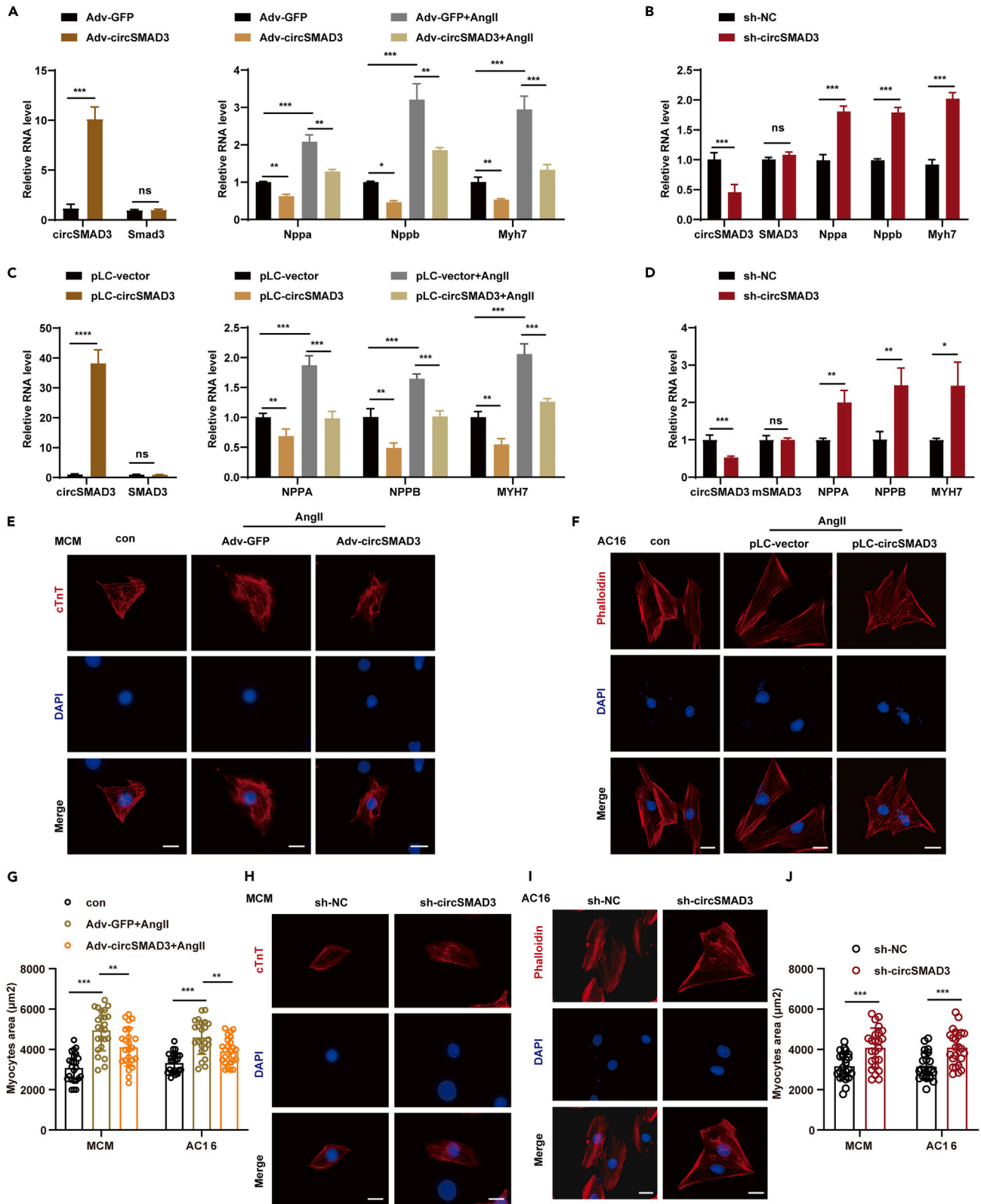


**Figure 3. CircSMAD3 is indispensable for anti-hypertrophy *in vitro***

(A–D) qPCR assays to detect the overexpression (A) and silence (B) efficiency of circSMAD3 and hypertrophic genes expression in RNA level in mouse primary cardiomyocytes and AC16. ( $n = 9$  per group).

(E and F) Phalloidin staining to cardiomyocyte area after circSMAD3 overexpression in mouse primary cardiomyocytes and AC16. Scale bar = 10  $\mu\text{m}$ .

(G) Quantification of cardiomyocytes area after circSMAD3 overexpression. ( $n = 24$  per group).

(H and I) Phalloidin staining to cardiomyocyte area after circSMAD3 silence in mouse primary cardiomyocytes and AC16. Scale bar = 10  $\mu\text{m}$ .

(J) Quantification of cardiomyocytes area after circSMAD3 silence. ( $n = 24$  per group).  $p$  values correspond to two-tailed unpaired  $t$  tests for A–D; two-way ANOVA with Tukey's multiple comparisons test for A and C; data are presented as the mean  $\pm$  SD of 3 independent experiments. \*\*\* $p < 0.001$ , \*\* $p < 0.01$ , \* $p < 0.05$ .

We also investigated the role of YBX1 in the effects of circSMAD3 on cardiac fibroblasts. These results demonstrated that YBX1 silencing reversed the repression of cardiac fibroblast migration and proliferation induced by circSMAD3 overexpression. Moreover, YBX1 overexpression reversed the activation of cardiac fibroblasts induced by circSMAD3 silencing (Figures S6A–S6N).

**CircSMAD3 suppresses the TGF $\beta$ /SMAD3 signaling pathway by promoting the interaction of YBX1 with SMAD3**

Next, we investigated whether YBX1 affected the TGF $\beta$ /SMAD3 signaling pathway. We overexpressed YBX1 in cardiac fibroblasts and measured the levels of SMAD3 and pSMAD3. The results demonstrated that YBX1 overexpression repressed the level of pSMAD3 induced by TGF $\beta$ 1, while it had no effect on the expression of SMAD3 (Figure 6A). The effect of YBX1 on SMAD3 and its phosphorylation were similar to that observed in HEK293T cells (Figure 6B). It has been reported that YBX1 acts as an antifibrotic factor by interacting with SMAD3 to obstruct the binding of SMAD3 with the p300 coactivator and interfere with the TGF $\beta$ /SMAD3 signaling pathway in regulating profibrotic gene transcription.<sup>19</sup> Hence, we hypothesized that circSMAD3 may promote interactions between YBX1 and SMAD3 to exert an anti-myocardial remodeling effect. The immunoprecipitation assay showed that circSMAD3 overexpression promoted the binding of YBX1 and SMAD3, whereas circSMAD3 silencing suppressed this interaction in cardiomyocytes and cardiac fibroblasts (Figures 6C and 6D). We truncated YBX1 and SMAD3 according to their respective domains to explore their specific binding domains. The results in HEK293T of the immunoprecipitation assay demonstrated that the MH1 domain of SMAD3 bound to YBX1, and the CTR domain of YBX1 interacted with SMAD3 (Figures 6E and 6F). Furthermore, circSMAD3 facilitated these two interactions (Figures 6G and 6H). We also performed a rescue assay to explore whether YBX1 participated in the role of SMAD3 phosphorylation mediated by circSMAD3, and found that YBX1 silencing reversed the repressive effect of SMAD3 phosphorylation induced by circSMAD3 overexpression (Figure 6I). In a dual-luciferase reporter assay, YBX1 significantly reduced the positive modulation of SMAD3 on the ACTA2 promoter; nevertheless, circSMAD3 facilitated this suppressive effect (Figure S7A). These data show that circSMAD3 promotes the binding of YBX1 with SMAD3 to repress SMAD3 phosphorylation.

YBX1 inhibits profibrotic gene expression as a negative transcription factor. However, the mechanism by which YBX1 modulates hypertrophic gene transcription remains unknown. Using the bioinformatics algorithm JASPAR,<sup>20</sup> we predicted that YBX1 has some binding sites in the promoter regions of hypertrophic genes, including *NPPA*, *NPPB*, and *MYH7* (Figures S7C and S7D). Hence, we constructed a fluorescent reporter gene vector with hypertrophy gene promoter region 2 kb YBX1 overexpression suppressed the luciferase activity (Figure S7B). The CHIP-qPCR and PCR results further verified the existence of binding sites for YBX1 in the promoter region of these genes (Figure S7D). Collectively, YBX1 not only acts as an anti-profibrotic factor but also serves as an antihypertrophic factor by directly repressing hypertrophic gene transcription.

**CircSMAD3 overexpression reduced cardiac remodeling *in vivo***

To assess the therapeutic effect of circSMAD3 in cardiac remodeling *in vivo*, we established a pressure overload model through TAC intervention and infected cells with AAV9-TnT-circSMAD3 or AAV9-TnT-GFP (Figures 7A and 7B). Compared with the AAV9-TnT-GFP group, circSMAD3 overexpression significantly ameliorated heart function, as detected by echocardiographic and hemodynamic measurements, as indicated by the values of  $dt/dt$  max,  $dt/dt$  min, ejection fraction, fractional shortening, and left ventricular anterolateral wall (Figures 7C–7H), decreased the gross heart and heart weight/tibia length ratio, and reversed cardiomyocyte hypertrophy and myocardial interstitial fibrosis in the circSMAD3 overexpression group (Figures 7I–7L). As expected, circSMAD3 overexpression reduced the expression of hypertrophic and profibrotic genes, promoted the expression of YBX1, and inhibited SMAD3 phosphorylation in the TAC group (Figures 7M–7O and S8).

Furthermore, we used another MI-induced heart failure model to elucidate the role of circSMAD3 (Figures 8A and 8B). Profibrotic and hypertrophic genes, including *Collagen I*, *Collagen III*, *ACTA2*, *NPPA*, *NPPB*, and *MYH7*, were significantly downregulated by circSMAD3 overexpression in both sham and MI groups (Figure 8C). Correspondingly, circSMAD3 improved the cardiac function in mice with MI, as indicated by the values of ejection fraction, fractional shortening,  $dP/dt$  max, and  $dP/dt$  min 28 days after MI (Figures 8D and 8E). Furthermore, circSMAD3 decreased the heart weight/tibia length ratio (Figure 8F) and ameliorated the infarction size and cardiac fibrosis (Figures 8G and 8H). Furthermore, circSMAD3 overexpression promoted the expression of YBX1 and inhibited SMAD3 phosphorylation in the TAC group (Figures 8I and 8J).

**DISCUSSION**

This study identified a factor, circSMAD3, that ameliorated cardiac hypertrophy and fibrosis and significantly improved cardiac function after heart failure. We observed that circSMAD3, derived from SMAD3 and regulated by Alu elements and DHX9, was downregulated during

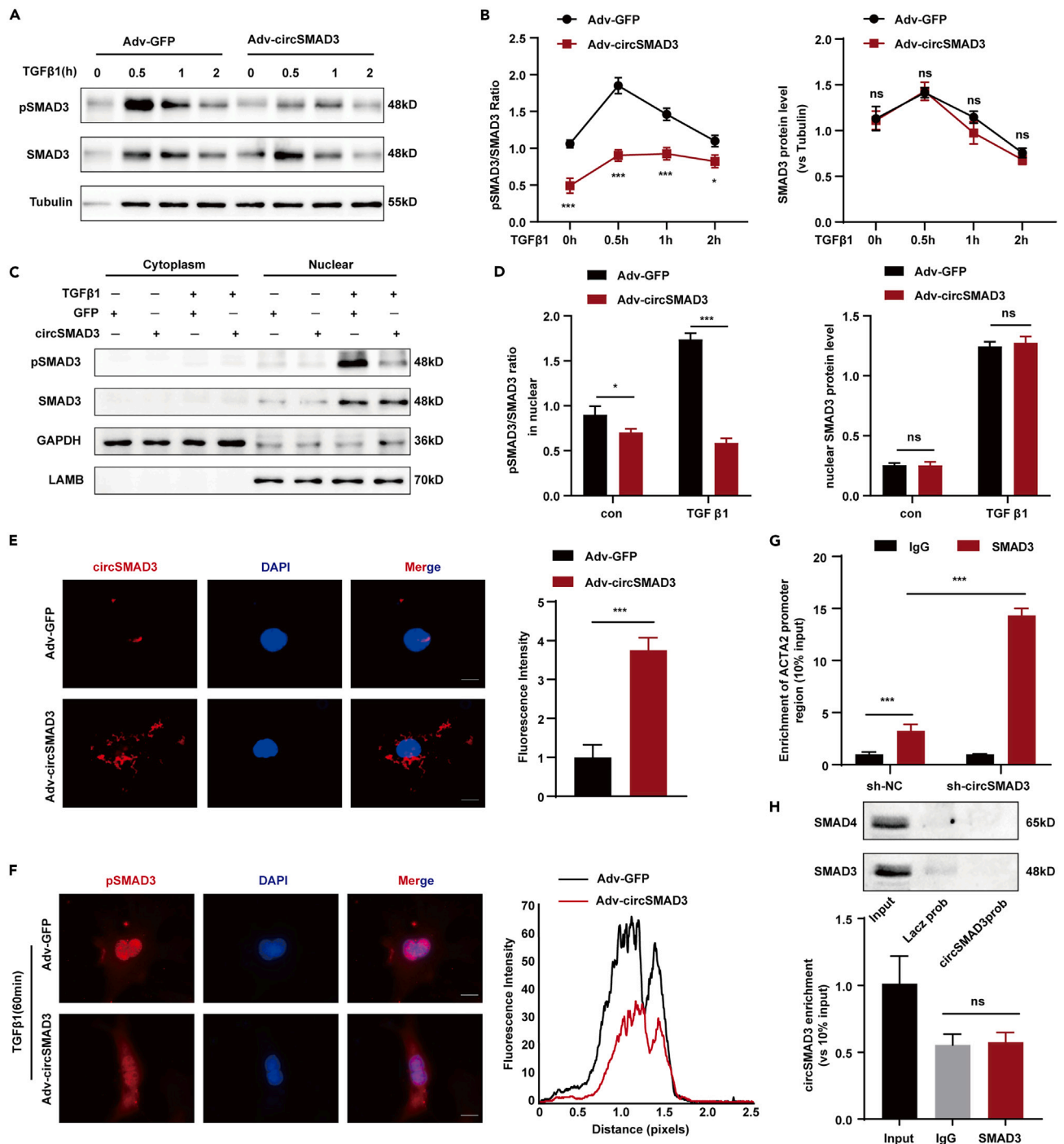


**Figure 4. circSMAD3 deactivates TGFβ/SMAD3 signaling pathway by inhibiting SMAD3 phosphorylation**

(A and B) Western blot to detect the change of pSMAD3 after circSMAD3 overexpression induced by TGFβ1 in cardiac fibroblasts. (n = 3 per group). (C and D) The change of pSMAD3 after circSMAD3 overexpression induced by TGFβ1 in the cytoplasm and nuclear of cardiac fibroblasts. (n = 3 per group). (E) FISH to detect the efficiency of circSMAD3 overexpression in cardiac fibroblasts. Scale bar = 10 μm. (n = 6 per group) (F) Immunofluorescence to detect the distribution of SMAD3 after circSMAD3 overexpression and TGFβ1 stimulation. Scale bar = 10 μm. (n = 6 per group). (G) circSMAD3 silence significantly promoted the binding of SMAD3 in ACTA2 gene promoter region in 2kb. (n = 6 per group). (H) UP, RNA pulldown to detect the interaction of SMAD3 and SMAD4 with circSMAD3. (n = 3 per group). DOWN, RNA immunoprecipitation to detect the enrichment of circSMAD3 by SMAD3. (n = 3 per group). p values correspond to one-way ANOVA with Tukey's multiple comparisons test for H; two-tailed unpaired t tests for E and F. two-way ANOVA with Tukey's multiple comparisons test for B, D, and G; Data are presented as the mean ± SD of 3 independent experiments. \*\*\*p < 0.001, \*\*p < 0.01, \*p < 0.05.

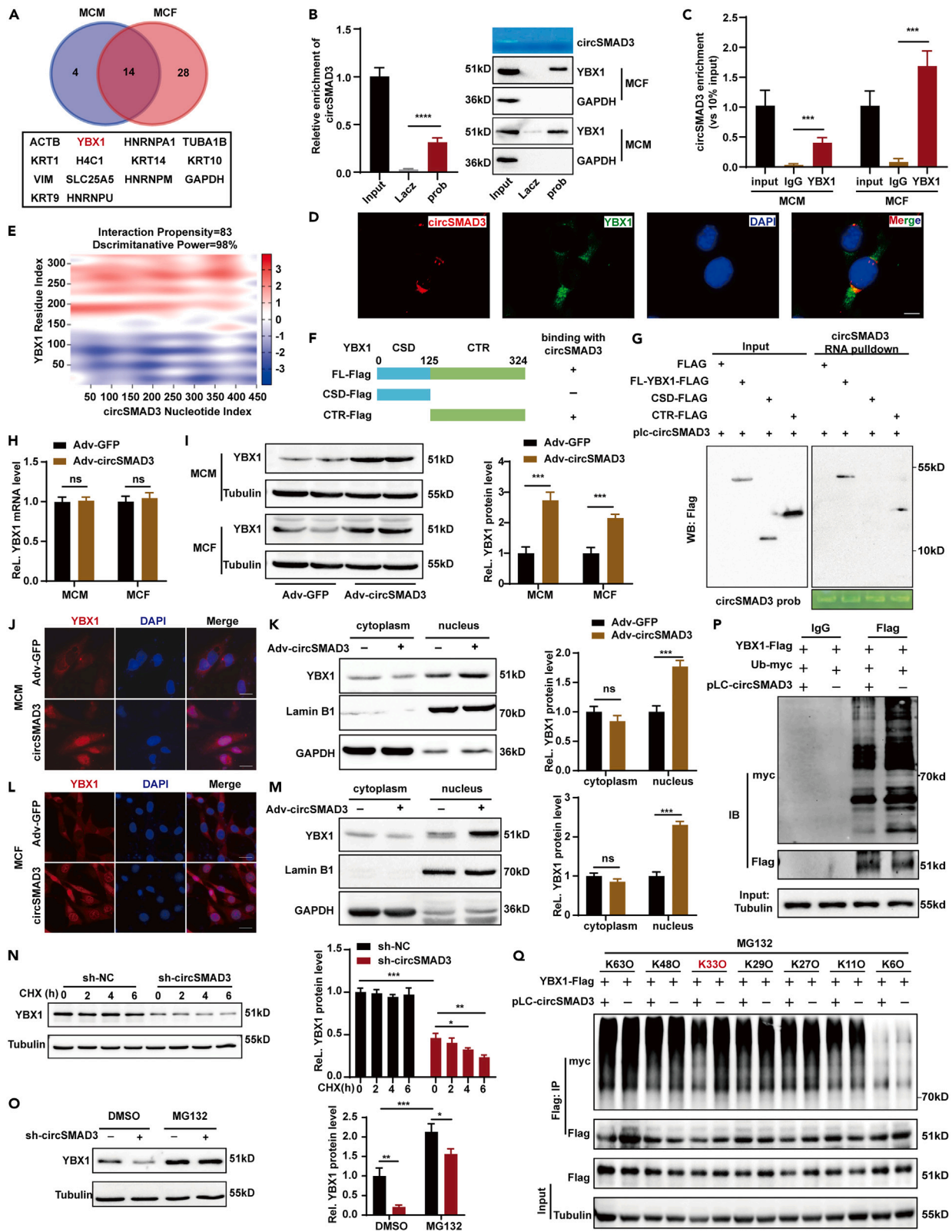


**Figure 5. CircSMAD3 interacts with YBX1 to suppresses its degradation by ubiquitination protease pathway**

(A) 14 proteins identified by mass spectrum in the circSMAD3 pulldown products.  
 (B) RNA pulldown assay shows the interaction of circSMAD3 and YBX1 in cardiomyocytes and cardiac fibroblasts. (n = 6 per group).  
 (C) RNA immunoprecipitation and qPCR revealed the enrichment of circSMAD3 by YBX1 in cardiomyocytes and cardiac fibroblasts. (n = 6 per group).  
 (D) Immunofluorescence staining showed the co-location of circSMAD3 and YBX1 in nuclear in cardiac fibroblasts. Scale bar = 10  $\mu$ m. (n = 12 per group).  
 (E) CatRapid to predict the interaction of circSMAD3 with YBX1.  
 (F and G) The schematic of circSMAD3 interacting with the c terminal region of YBX1. (n = 3 per group).  
 (H and I) RNA and Protein level of YBX1 in response to the overexpression of circSMAD3 in cardiomyocytes and cardiac fibroblasts. (n = 6 per group).  
 (J–M) Immunofluorescence and Cytoplasmic and nuclear protein extraction assay to detect the distribution of YBX1 in response to circSMAD3 overexpression in cardiomyocytes and cardiac fibroblasts. Scale bar = 50  $\mu$ m. (n = 6 per group).  
 (N and O) MG132, rather than CHX reversed the decrease of YBX1 induced by circSMAD3 decline. (n = 6 per group).  
 (P) Immunoprecipitation assay to detect the interaction intensity of YBX1 and ubiquitin with or without circSMAD3. (n = 6 per group).  
 (Q) Immunoprecipitation assay to detect the ubiquitination sites of YBX1 promoted by circSMAD3. (n = 4 per group). p values correspond to two-tailed unpaired t tests for G, H, J and L; one-way ANOVA with Tukey's multiple comparisons test for B and C; two-way ANOVA with Tukey's multiple comparisons test for M and N; data are presented as the mean  $\pm$  SD of 3–4 independent experiments. \*\*\*p < 0.001, \*\*p < 0.01, \*p < 0.05.

cardiac remodeling and heart failure. Mechanistically, circSMAD3 interacts with YBX1 and maintains its stability to repress transcription. It also enhanced the interaction of YBX1 with SMAD3 and inhibited SMAD3 phosphorylation to suppress transcriptional modulation of the TGF $\beta$ /SMAD3 signaling pathway. Therefore, this study indicates that circSMAD3 may be a potent therapeutic target for restoring cardiac function and preventing cardiac remodeling and heart failure.

The TGF $\beta$  signaling pathways, which include classical and nonclassical pathways, are critical in various pathophysiological processes, including cardiac remodeling and heart failure. However, many efforts targeting TGF $\beta$  to treat remodeling have been unsuccessful because of its side effects resulting from its multifunctionality. Therefore, targeting downstream effectors may be a promising approach for developing treatments for heart failure. We discovered that circSMAD3 interacts with YBX1 and enhances the interaction of YBX1 with SMAD3 to repress SMAD3 phosphorylation, eventually decreasing the function of the TGF- $\beta$ /SMAD3 signaling pathway. This effect ensures the functionality of circSMAD3, which improves cardiac remodeling and heart failure. Moreover, these results demonstrate that finding a treatment for heart failure from the downstream effector of the TGF $\beta$  signaling pathway may be promising.

Interaction with proteins is a critical mechanism by which non-coding RNAs, including circRNAs, exert their function.<sup>21,22</sup> YBX1 has a highly conserved cold shock domain with broad nucleic acid-binding properties and participates in transcriptional regulation,<sup>23,24</sup> translation, pre-mRNA splicing<sup>25</sup> and modification.<sup>26,27</sup> YBX1 acts as a bidirectional transcriptional regulator of cardiovascular disease. In MI, it is a positive transcription factor that modulates the transcription of cycling A2 and cycling B1, and then mediates cardiomyocyte proliferation and cardiac regeneration.<sup>18</sup> In vascular diseases, YBX1 serves as a negative factor that inhibits ACTA2 transcription by directly binding to its promoter.<sup>17,28</sup> Furthermore, YBX1 serves as an antifibrotic factor by its direct or indirect function; it can bind with interferon- $\gamma$  reaction element (IgRE) directly to suppress COL1A2 transcription. It also binds with SMAD3 to obstruct the interaction of SMAD3 with the p300 coactivator bound to the TbRE, and then antagonizes the TGF- $\beta$ /SMAD3 signaling pathway in regulating COL1A2 transcription.<sup>19</sup> These reports suggest that YBX1 has a significant effect on cardiac remodeling. Therefore, YBX1, a transcriptional regulation-repressive factor, has attracted substantial attention.

This study demonstrates that YBX1 acts as an antifibrotic factor that negatively regulates profibrotic gene expression and represses cardiac fibroblast activation. However, it also inhibits cardiomyocyte hypertrophy by binding to the hypertrophic gene promoter region. Additionally, YBX1 degradation via the ubiquitin–proteasome pathway has been reported in patients with MI. However, unlike the ubiquitination degradation of YBX1 induced by circRNA NFIX in MI, circSMAD3 maintained YBX1 stability by protecting it from the ubiquitin–proteasome pathway and promoting its activation. These two opposing modulation patterns demonstrate the complexity of circRNAs in the pathophysiological regulation. In summary, our findings indicate that circSMAD3 is a critical epigenetic regulator of cardiac fibrosis and hypertrophy. This presents a mechanism through which circSMAD3 regulates cardiac myofibroblast activation and is indispensable for anti-hypertrophy, indicating that circSMAD3 is a promising target for heart failure treatment.

**Limitations of the study**

There are still some limitations in this study. First, we only explored the role of circSMAD3 in cardiac remodeling and heart failure by the means of adeno-associated virus, rather than applying circSMAD3 transgenic mice. Second, despite we verified the roles of YBX1 in cardiac hypertrophy and cardiac fibrosis *in vitro*, we did not verify its function *in vivo*. Therefore, we will further solve those limitations in the future.

**STAR★METHODS**

Detailed methods are provided in the online version of this paper and include the following:

- KEY RESOURCES TABLE
- RESOURCE AVAILABILITY
  - Lead contact

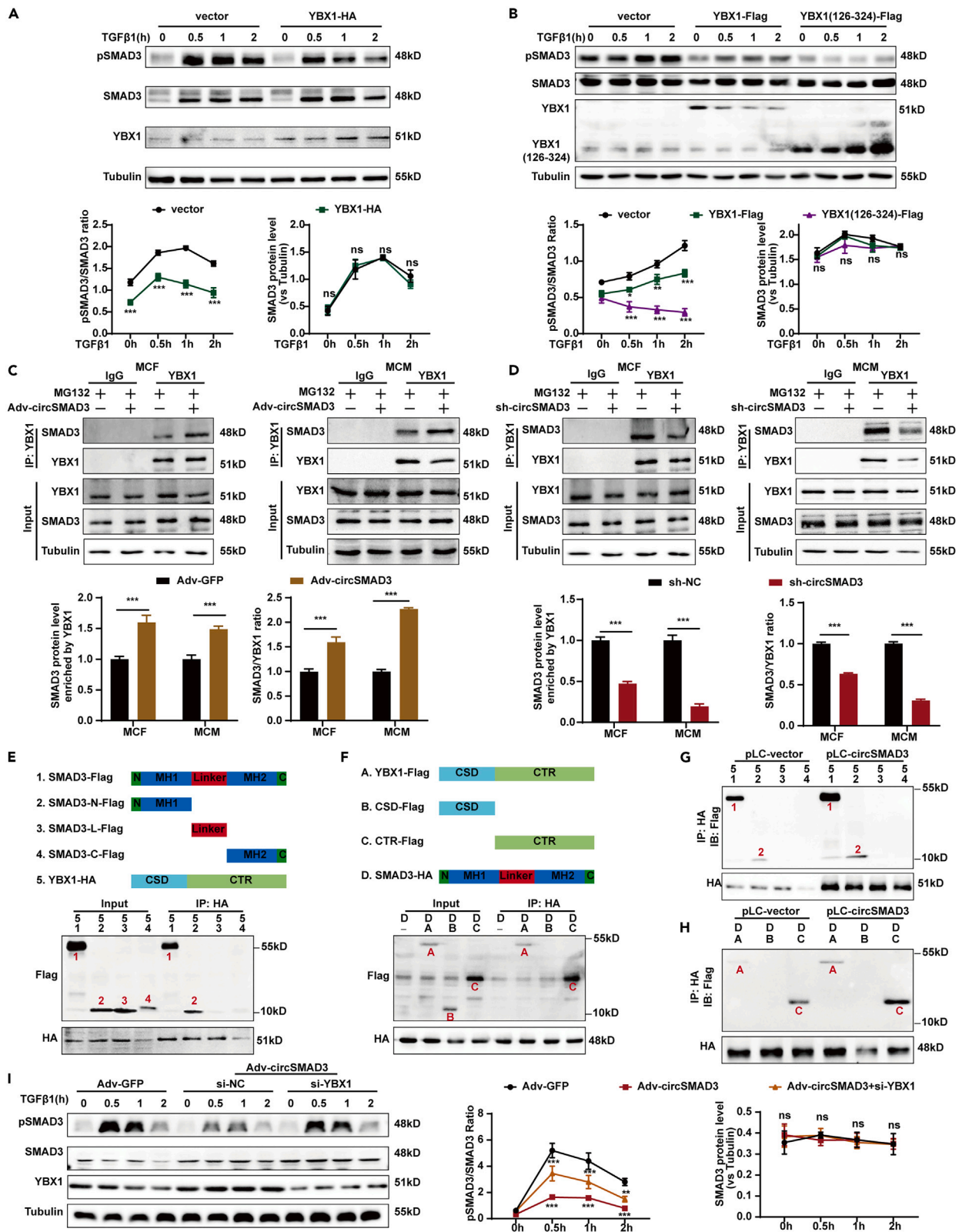


**Figure 6. CircSMAD3 suppresses TGFβ/SMAD3 signaling pathway by promoting the interaction of YBX1 and SMAD3**

(A) The change of pSMAD3 after YBX1 overexpression in cardiac fibroblasts stimulated by TGFβ1. (n = 3 per group).  
 (B) The change of pSMAD3 after YBX1 and its C terminal overexpression in HEK293T stimulated by TGFβ1. (n = 3 per group).  
 (C and D) Immunoprecipitation assay showed that overexpression (C) or silence (D) of circSMAD3 influenced the binding of YBX1 with SMAD3 in cardiac fibroblasts and cardiomyocytes. (n = 3 per group).  
 (E) Truncated assay to verified the specific domain of SMAD3 interacting with YBX1. (n = 3 per group).  
 (F) Truncated assay to verified the specific domain of YBX1 interacting with SMAD3. (n = 3 per group).  
 (G) CircSMAD3 overexpression promoted MH1 domain of SMAD3 interacting with YBX1. (n = 3 per group).  
 (H) CircSMAD3 overexpression promoted CTR domain of YBX1 interacting with SMAD3. (n = 3 per group).  
 (I) YBX1 silence reversed the decline effect of pSMAD3 induced by circSMAD3 overexpression in cardiac fibroblasts stimulated by TGFβ1. p values correspond to two-way ANOVA with Tukey's multiple comparisons test for A, B, I, J and L; two-tailed unpaired t tests for C and D; data are presented as the mean ± SD of 3 independent experiments. \*\*\*p < 0.001, \*\*p < 0.01, \*p < 0.05.

- Materials availability
- Data and code availability
- **EXPERIMENTAL MODEL AND STUDY PARTICIPANT DETAILS**
  - Animal administration and ethics statement
- **METHOD DETAILS**
  - Cell culture and treatment
  - RNA isolation, quantitative RT-PCR and PCR
  - Protein extraction and western blotting
  - Rnase R digestion
  - Fluorescence *in situ* hybridization (FISH)
  - Construction of overexpression vector
  - Package and infection of adenovirus and adeno-associated virus type 9
  - Immunofluorescence analysis
  - Isolation of primary cardiomyocytes and cardiac fibroblasts
  - Cell area measure
  - CCK8 assay
  - Wound healing assay
  - 5-Ethynyl-2'-deoxyuridine (EdU) assay
  - Pull-down assay with biotinylated circSMAD3 probe
  - RNA immunoprecipitation (RIP)
  - Luciferase reporter assay
  - Chromatin immunoprecipitation (ChIP)
  - Transverse aortic constriction (TAC)
  - Myocardial infraction (MI)
  - Echocardiography
  - Data analysis
- **QUANTIFICATION AND STATISTICAL ANALYSIS**

**SUPPLEMENTAL INFORMATION**

Supplemental information can be found online at <https://doi.org/10.1016/j.isci.2024.110200>.

**ACKNOWLEDGMENTS**

This study was supported by grants from the National Natural Science Foundation of China (Grant numbers: 82170392, 81974047, and 81790624), the National Key Research and Development Program of China (Grant numbers: 2021YFC2500600, 2021YFC2500604), and the Hubei Key Research and Development Program (No. 2021BCA121). We thank Prof. Zefeng Wang (CAS Key Lab for Computation Biology) and Prof. Mian Wu (CAS Key Laboratory of Innate Immunity and Chronic Disease) for providing the GFP split-translation reporter system.

**AUTHOR CONTRIBUTIONS**

H.D. and J.Y. designed the study. S.M., X.M., Y.Q., L.Z., Q.X., and M.W. performed the experiments. S.M., X.M., J.W., K.Z., and C.C. analyzed the data and provided some experimental materials. S.M. and H.D. wrote the draft of the manuscript. All authors in this study have read and approved the article.

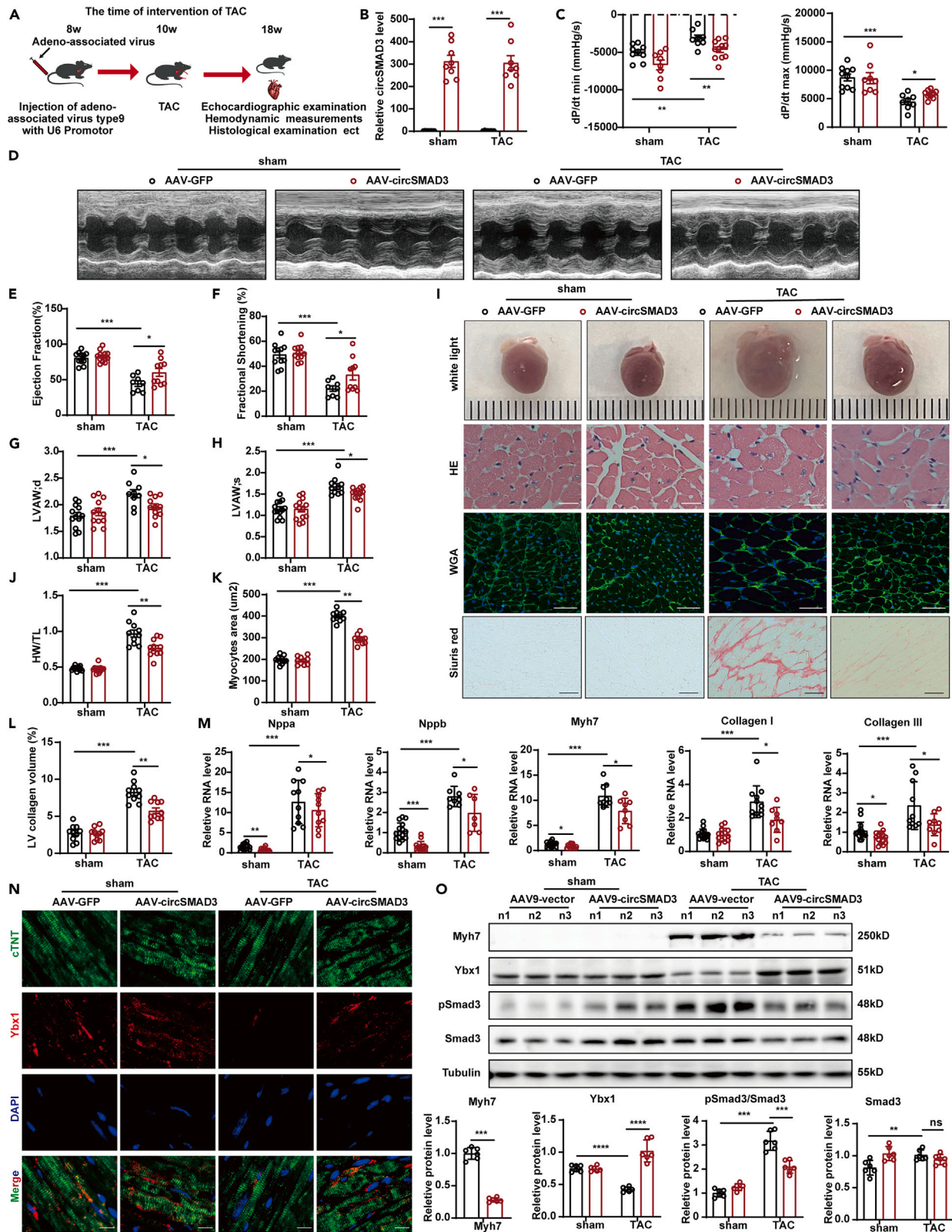


**Figure 7. Overexpression of circSMAD3 ameliorates cardiac hypertrophy and improves cardiac function in vivo**

- (A) The schematic of transverse aortic constriction operation time.
- (B) The expression of circSMAD3 in each group. (n = 8 per group).
- (C) The indicator of hemodynamic measurement in each group. (n = 10 per group).
- (D–H) Echocardiographic examination to detect the values of cardiac function. (n = 8–13 per group).
- (I) The HE staining, WGA staining and Sirius red staining in the heart to detect the cardiomyocyte area and myocardial interstitial fibrosis in each group. Scale bar = 10 μm in HE staining, WGA staining and Sirius red staining.
- (J) HW/TL ratio in each group. (n = 10 per group).
- (K) The value of myocytes area in each group. (n = 10 per group).
- (L) The indicators of LV collagen volume in each group. (n = 10 per group).
- (M) qPCR to detect the transcriptional level of hypertrophic genes and profibrotic genes. (n = 10–15 per group).
- (N) Immunoprecipitation to detect the expression of YBX1 in each group. cTnT was the marker of cardiomyocytes. Scale bar = 10 μm.
- (O) Western blot to detect the expression of Myh7, Ybx1 and pSMAD3 in each group. (n = 6 per group). p values correspond to two-way ANOVA with Tukey's multiple comparisons test in this part; Data are shown as mean ± SEM. \*\*\*p < 0.001, \*\*p < 0.01, \*p < 0.05.

**DECLARATION OF INTERESTS**

The authors declare no competing interests.

Received: February 14, 2024

Revised: April 18, 2024

Accepted: June 3, 2024

Published: June 8, 2024

**REFERENCES**

1. Baman, J.R., and Ahmad, F.S. (2020). Heart Failure. *JAMA* 324, 1015. <https://doi.org/10.1001/jama.2020.13310>.
2. Dunlay, S.M., Roger, V.L., and Redfield, M.M. (2017). Epidemiology of heart failure with preserved ejection fraction. *Nat. Rev. Cardiol.* 14, 591–602. <https://doi.org/10.1038/nrcardio.2017.65>.
3. Hou, J., and Kang, Y.J. (2012). Regression of pathological cardiac hypertrophy: signaling pathways and therapeutic targets. *Pharmacol. Ther.* 135, 337–354. <https://doi.org/10.1016/j.pharmthera.2012.06.006>.
4. Lam, C.S.P., Voors, A.A., de Boer, R.A., Solomon, S.D., and van Velthuisen, D.J. (2018). Heart failure with preserved ejection fraction: from mechanisms to therapies. *Eur. Heart J.* 39, 2780–2792. <https://doi.org/10.1093/eurheartj/ehy301>.
5. Bujak, M., and Frangogiannis, N.G. (2007). The role of TGF-beta signaling in myocardial infarction and cardiac remodeling. *Cardiovasc. Res.* 74, 184–195. <https://doi.org/10.1016/j.cardiores.2006.10.002>.
6. Meng, X.M., Nikolic-Paterson, D.J., and Lan, H.Y. (2016). TGF-β: the master regulator of fibrosis. *Nat. Rev. Nephrol.* 12, 325–338. <https://doi.org/10.1038/nrneph.2016.48>.
7. Schafer, S., Viswanathan, S., Widjaja, A.A., Lim, W.W., Moreno-Moral, A., DeLaughter, D.M., Ng, B., Patone, G., Chow, K., Khin, E., et al. (2017). IL-11 is a crucial determinant of cardiovascular fibrosis. *Nature* 552, 110–115. <https://doi.org/10.1038/nature24676>.
8. Ebbesen, K.K., Hansen, T.B., and Kjems, J. (2017). Insights into circular RNA biology. *RNA Biol.* 14, 1035–1045. <https://doi.org/10.1080/15476286.2016.1271524>.
9. Vicens, Q., and Westhof, E. (2014). Biogenesis of Circular RNAs. *Cell* 159, 13–14. <https://doi.org/10.1016/j.cell.2014.09.005>.
10. Hall, I.F., Climent, M., Quintavalle, M., Farina, F.M., Schorn, T., Zani, S., Carullo, P., Kunderfranco, P., Civilini, E., Condorelli, G., and Elia, L. (2019). Circ-Lrp6, a Circular RNA Enriched in Vascular Smooth Muscle Cells, Acts as a Sponge Regulating miRNA-145 Function. *Circ. Res.* 124, 498–510. <https://doi.org/10.1161/CIRCRESAHA.118.314240>.
11. Li, Q., Wang, Y., Wu, S., Zhou, Z., Ding, X., Shi, R., Thorne, R.F., Zhang, X.D., Hu, W., and Wu, M. (2019). CircACC1 Regulates Assembly and Activation of AMPK Complex under Metabolic Stress. *Cell Metabol.* 30, 157–173.e7. <https://doi.org/10.1016/j.cmet.2019.05.009>.
12. Li, Z., Huang, C., Bao, C., Chen, L., Lin, M., Wang, X., Zhong, G., Yu, B., Hu, W., Dai, L., et al. (2015). Exon-intron circular RNAs regulate transcription in the nucleus. *Nat. Struct. Mol. Biol.* 22, 256–264. <https://doi.org/10.1038/nsmb.2959>.
13. Legnini, I., Di Timoteo, G., Rossi, F., Morlando, M., Briganti, F., Sthandier, O., Fatica, A., Santini, T., Andronache, A., Wade, M., et al. (2017). Circ-ZNF609 Is a Circular RNA that Can Be Translated and Functions in Myogenesis. *Mol. Cell* 66, 22–37.e9. <https://doi.org/10.1016/j.molcel.2017.02.017>.
14. Xiao, M.S., Ai, Y., and Wilusz, J.E. (2020). Biogenesis and Functions of Circular RNAs Come into Focus. *Trends Cell Biol.* 30, 226–240. <https://doi.org/10.1016/j.tcb.2019.12.004>.
15. Lee, T., Paquet, M., Larsson, O., and Pelletier, J. (2016). Tumor cell survival dependence on the DHX9 DEXH-box helicase. *Oncogene* 35, 5093–5105. <https://doi.org/10.1038/onc.2016.52>.
16. Armaos, A., Colantoni, A., Proietti, G., Rupert, J., and Tartaglia, G.G. (2021). catRAPID omics v2.0: going deeper and wider in the prediction of protein-RNA interactions. *Nucleic Acids Res.* 49, W72–W79. <https://doi.org/10.1093/nar/gkab393>.
17. Yu, J., Wang, W., Yang, J., Zhang, Y., Gong, X., Luo, H., Cao, N., Xu, Z., Tian, M., Yang, P., et al. (2022). LncRNA PSR Regulates Vascular Remodeling Through Encoding a Novel Protein Arteridin. *Circ. Res.* 131, 768–787. <https://doi.org/10.1161/CIRCRESAHA.122.321080>.
18. Huang, S., Li, X., Zheng, H., Si, X., Li, B., Wei, G., Li, C., Chen, Y., Chen, Y., Liao, W., et al. (2019). Loss of Super-Enhancer-Regulated circRNA Nfix Induces Cardiac Regeneration After Myocardial Infarction in Adult Mice. *Circulation* 139, 2857–2876. <https://doi.org/10.1161/CIRCULATIONAHA.118.038361>.
19. Higashi, K., Inagaki, Y., Fujimori, K., Nakao, A., Kaneko, H., and Nakatsuka, I. (2003). Interferon-gamma interferes with transforming growth factor-beta signaling through direct interaction of YB-1 with Smad3. *J. Biol. Chem.* 278, 43470–43479. <https://doi.org/10.1074/jbc.M302339200>.
20. Fornes, O., Castro-Mondragon, J.A., Khan, A., van der Lee, R., Zhang, X., Richmond, P.A., Modi, B.P., Correard, S., Gheorghe, M., Baranasic, D., et al. (2020). JASPAR 2020: update of the open-access database of transcription factor binding profiles. *Nucleic Acids Res.* 48, D87–D92. <https://doi.org/10.1093/nar/gkz1001>.
21. Gomes, C.P.C., Schroen, B., Kuster, G.M., Robinson, E.L., Ford, K., Squire, I.B., Heymans, S., Martelli, F., Emanuelli, C., and Devaux, Y.; EU-CardioRNA COST Action CA17129 (2020). Regulatory RNAs in Heart Failure. *Circulation* 141, 313–328. <https://doi.org/10.1161/CIRCULATIONAHA.119.042474>.
22. Holdt, L.M., Kohlmaier, A., and Teupser, D. (2018). Molecular roles and function of circular RNAs in eukaryotic cells. *Cell. Mol. Life Sci.* 75, 1071–1098. <https://doi.org/10.1007/s00018-017-2688-5>.
23. Xu, J., Ji, L., Liang, Y., Wan, Z., Zheng, W., Song, X., Gorshkov, K., Sun, Q., Lin, H., Zheng, X., et al. (2020). CircRNA-SORE mediates sorafenib resistance in hepatocellular carcinoma by stabilizing YBX1. *Signal Transduct. Targeted Ther.* 5, 298. <https://doi.org/10.1038/s41392-020-00375-5>.
24. Chen, Q., Wang, H., Li, Z., Li, F., Liang, L., Zou, Y., Shen, H., Li, J., Xia, Y., Cheng, Z., et al. (2022). Circular RNA ACTN4 promotes intrahepatic cholangiocarcinoma

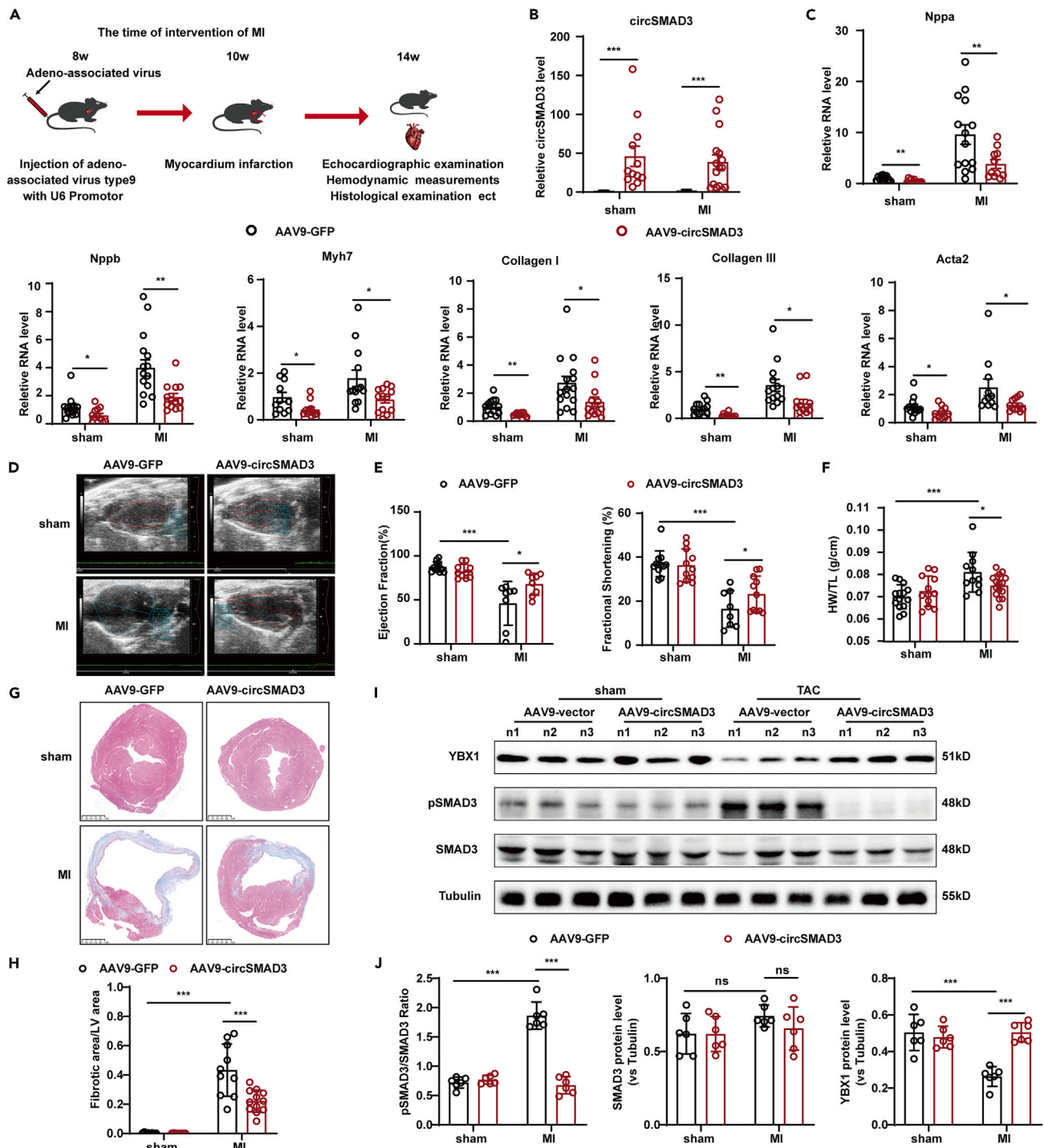


**Figure 8. CircSMAD3 overexpression ameliorated cardiac remodeling in murine heart failure models induced by MI**

(A) The schematic of myocardium infarction operation time.

(B) The expression of circSMAD3 in each group. (n = 10–15 per group).

(C) qPCR to detect the transcriptional level of hypertrophic genes and fibrosis genes (n = 10–15 per group).

(D and E) Echocardiographic examination to detect the cardiac function (n = 8–11 per group).

(F) HW/TL ratio in each group (n = 11–15 per group).

(G and H) The changes of fibrosis area in heart undergoing MI. (n = 10–12 per group). Scale bar = 1 mm.

(I and J) Western blot to detect the expression of Myh7, Ybx1 and pSMAD3 in each group. (n = 6 per group). p values correspond to two-way ANOVA with Tukey's multiple comparisons test in this part; Data are shown as mean ± SEM. \*\*\*p < 0.001, \*\*p < 0.01, \*p < 0.05.

- progression by recruiting YBX1 to initiate FZD7 transcription. *J. Hepatol.* 76, 135–147. <https://doi.org/10.1016/j.jhep.2021.08.027>.
25. Perner, F., Schnoeder, T.M., Xiong, Y., Jayavelu, A.K., Mashamba, N., Santamaria, N.T., Huber, N., Todorova, K., Hatton, C., Perner, B., et al. (2022). YBX1 mediates translation of oncogenic transcripts to control cell competition in AML. *Leukemia* 36, 426–437. <https://doi.org/10.1038/s41375-021-01393-0>.
26. Jayavelu, A.K., Schnöder, T.M., Perner, F., Herzog, C., Meiler, A., Krishnamoorthy, G., Huber, N., Mohr, J., Edelmann-Stephan, B., Austin, R., et al. (2020). Splicing factor YBX1 mediates persistence of JAK2-mutated neoplasms. *Nature* 588, 157–163. <https://doi.org/10.1038/s41586-020-2968-3>.
27. Feng, M., Xie, X., Han, G., Zhang, T., Li, Y., Li, Y., Yin, R., Wang, Q., Zhang, T., Wang, P., et al. (2021). YBX1 is required for maintaining myeloid leukemia cell survival by regulating BCL2 stability in an m6A-dependent manner. *Blood* 138, 71–85. <https://doi.org/10.1182/blood.2020009676>.
28. Becker, N.A., Kelm, R.J., Jr., Vrana, J.A., Getz, M.J., and Maher, L.J., 3rd (2000). Altered sensitivity to single-strand-specific reagents associated with the genomic vascular smooth muscle alpha-actin promoter during myofibroblast differentiation. *J. Biol. Chem.* 275, 15384–15391. <https://doi.org/10.1074/jbc.M909687199>.

## STAR★METHODS

## KEY RESOURCES TABLE

REAGENT or RESOURCE	SOURCE	IDENTIFIER
Chemicals, peptides, and recombinant proteins		
Human Angiotensin II	MedChemExpress	Cat# HY-13948
Mouse TGF- $\beta$ 1	MedChemExpress	Cat# HY-P70648
MG-132	MedChemExpress	Cat# HY-13259
Cycloheximide (CHX)	MedChemExpress	Cat# HY-12320
Actinomycin D (ActD)	MedChemExpress	Cat# HY-17559
Rhodamine Phalloidin	Abclonal	Cat# RM02835
Critical commercial assays		
Cell-Light EdU Apollo567 <i>In Vitro</i> Kit	Riobio	Cat# C10310-1
TSA System	Servicebio	Cat# G1226-50T
Magna RIP Kit	Millipore	Cat# RIP-12RXN
ChIP Kit	Beyotime Bio	Cat# P2078
Antibody		
$\alpha$ -Tubulin	Abclonal	Cat# AC025; RRID:AB_2768344
GAPDH	Abclonal	Cat# AC002; RRID:AB_2736879
CD31	Abcam	Cat# ab28364; RRID:AB_726362
cTNT	Abcam	Cat# ab209813; RRID:AB_2938619/Cat# ab8295; RRID:AB_306445
Vimentin	Abcam	Cat# ab16700; RRID:AB_443435
Lamin B (LamB)	Proteintech	Cat# 66095-1-Ig; RRID:AB_11232208
GFP	Proteintech	Cat# 66002-1-Ig; RRID:AB_11182611
Collagen I	Proteintech	Cat# 14695-1-AP; RRID:AB_2082037
Collagen III	Proteintech	Cat# 22734-1-AP; RRID:AB_2879158
ACTA2	Abclonal	Cat# A17910; RRID:AB_2861755
SMAD3	Abcam	Cat# ab40854; RRID:AB_777979
pSMAD3	Abcam	Cat# ab52903; RRID:AB_882596
YBX1	Proteintech	Cat# 20339-1-AP; RRID:AB_10665424
FLAG	Proteintech	Cat# 66008-4-Ig; RRID:AB_2918475
MYC	Proteintech	Cat# 16286-1-AP; RRID:AB_11182162
MYH7	Proteintech	Cat# 22280-1-AP; RRID:AB_2736821
HRP Anti-Digoxigenin	Abcam	Cat# ab51949; RRID:AB_869468

## RESOURCE AVAILABILITY

## Lead contact

Further information and requests for resources should be directed to and will be fulfilled by the lead contact, Prof. Hu Ding ([dingo8369@163.com](mailto:dingo8369@163.com)).

## Materials availability

This study did not generate unique reagents.

## Data and code availability

Data reported in this paper will be shared by the [lead contact](#) upon request. This paper does not report original code. Any additional information required to reanalyze the data reported in this paper is available from the [lead contact](#) upon request.

## EXPERIMENTAL MODEL AND STUDY PARTICIPANT DETAILS

### Animal administration and ethics statement

Seven-week-old C57 B/J male mice purchased from GemPharmatech Co., Ltd. (Jiangsu, China) were administered adeno-associated virus serotype 9 (AAV9) with cardiac troponin T (TnT) or the U6 promoter via the tail vein. After 3 weeks, the mice were intraperitoneally anesthetized with xylazine (5 mg/kg) and ketamine (80 mg/kg) (Sigma, USA) to induce TAC or MI, establishing a heart failure model. The same preparation was performed for another 8 weeks for TAC or 4 weeks for MI, and the cardiac function of the mice was assessed using echocardiography in M or B mode. At the end of the experiment, all mice were euthanized by intraperitoneal injection of xylazine (5 mg/kg) and ketamine (80 mg/kg). All mice were maintained and studied using protocols approved by the Committee on the Ethics of Animal Experiments of the Animal Research Committee of Tongji Medical College and in accordance with the National Institutes of Health Guide for the Care and Use of Laboratory Animals. ([2022] IACUC Number3280).

## METHOD DETAILS

### Cell culture and treatment

The cell lines of cardiomyocyte, AC16 were purchased from the American Type Culture Collection (ATCC, Manassas, VA, USA). The cells, including Mouse primary cardiomyocytes, AC16 and mouse primary cardiac fibroblasts, were cultured in Dulbecco's Modified Eagle's Medium (DMEM) containing 10% fetal bovine serum (FBS, GIBCO, Brazil) in a humidified atmosphere at 37°C with 5% CO<sub>2</sub>. Angiotensin II was dissolved in dimethyl sulfoxide at 1 mM concentration. TGFβ1 was dissolved in deionized water at a concentration of 10 ng/μL. When stimulated, the cells were cultured in serum-free DMEM for 6 h following Angiotensin II at 1 μM for another 24 h circSMAD3 siRNAs are designed and synthesized by RiboBio (Guangzhou, China), and were transfected at a final concentration of 50nM using Lipofectamine2000 (Invitrogen, USA), following the manufacturer's protocol. The sequences of siRNAs are shown in the [Table S3](#).

### RNA isolation, quantitative RT-PCR and PCR

We extracted total RNA from cultured cells by using TRIzol reagent (Takara, DaLian, China) in accordance with the manufacturer's instructions. Its purity and quantity were detected using NanoDrop ND-2000 (NanoDrop Thermo, Wilmington, DE, USA). The circRNA was reverse-transcribed using random primers via the Takara system. Thereafter, real-time PCR was performed using the Vazyme system on the 7900HT FAST Real-time PCR System (Life Technologies, Carlsbad, CA, USA). Using the formula  $2^{-\Delta\Delta C_t}$ , we calculated the levels of target genes according to the cycle threshold (Ct) values in comparison with a reference gene. GAPDH mRNA and U6 snRNA were used as references for mRNA and circRNA, respectively.

### Protein extraction and western blotting

Cells were lysed in ice-cold immunoprecipitation lysis buffer (Beyotime Bio, Shanghai, China), incubated with shaking at 4°C for 20 min, and subsequently centrifuged for 15 min (12,000×g, 4°C). After collecting the supernatant, the protein concentration was calculated using the Pierce Bicinchoninic Acid Protein Assay Kit (Thermo Fisher Scientific, Rockford, IL, USA). The protein levels were normalized by probing the same blots with α-Tubulin (AC025, Abclonal, Wuhan, China) and GAPDH antibodies (AC002, Abclonal, Wuhan, China). The primary antibodies used in this study were Collagen I (14695-1-AP, Proteintech, Wuhan, China), Collagen III (22734-1-AP, Proteintech, Wuhan, China), ACTA2 (A17910, Abclonal, Wuhan, China), MYH7 (A22140, Abclonal, Wuhan, China), YBX1 (A7704, Abclonal, Wuhan, China), Ubiquitin (10201-2-AP, Proteintech, Wuhan, China), SMAD3 (ab208182, Abcam, USA), pSMAD3 (ab52903, Abcam, USA), Flag (66008-4-Ig, Proteintech, Wuhan, China), HA (66006-2-Ig, Proteintech, Wuhan, China), Myc (60003-2-Ig, Proteintech, Wuhan, China).

### Rnase R digestion

Total RNA was extracted according to the protocol above. For the Rnase R digestion, 1 μg RNA was added to the north tube with 1U Rnase R and 2μL 10× buffer according to the kit from Epigenetic company (USA), and incubated at 37°C for 30 min the remaining RNA were circRNA and extracted as the protocol above.

### Fluorescence *in situ* hybridization (FISH)

Dig-labeled probes were specific to the junction sequence of circSMAD3. The probe was synthesized by Sangon Biotech (Shanghai, China), and the signals of the probes were detected by TSA system (G1236, Servicebio, Wuhan, China) according to the manufacturer's instructions. The HRP Anti-Digoxigenin was from Abcam company (ab51949, USA). The images were acquired on Lei TCS SP8 Laser Scanning Confocal Microscope (Leica Microsystems, Mannheim, Germany). The sequence of prob were listed in [Table S4](#).

### Construction of overexpression vector

The circSMAD3 overexpression plasmid was conducted on the base of pLC5 plasmid by GENESEED company (Guangzhou, China). In brief, the full sequence of circSMAD3 was amplified by PCR, cut by EcoRI and BamHI, and then connected into pLC5-vector. after being connected, circSMAD3 overexpression was sequenced to detect the accuracy of it by sanger sequencing. The efficiency of circSMAD3

overexpression was detected by qPCR. The plasmids to detect the role of ALU element were constructed based on pcDNA3.1 vector by Crys-tecpharma company (Guangzhou, China).

In this study, these vectors, including YBX1-flag, YBX1-HA, YBX1-CSD-flag, YBX1-CTR-Flag, SMAD3-HA, SMAD3-Flag, SMAD3-N-Flag, SMAD3-L-Flag, SMAD3-C-Flag, UB-Myc, UB-Myc (K63O), UB-Myc (K48O), UB-Myc (K33O), UB-Myc (K29O), UB-Myc (K27O), UB-Myc (K11O), and UB-Myc (K6O), were constructed by Aoke Biocompany (Wuhan, China). Those vectors were performed according to the experiments.

### Package and infection of adenovirus and adeno-associated virus type 9

For the alteration of circSMAD3 expression *in vitro*, circSMAD3 overexpression adenovirus and sh-circSMAD3 adenovirus were packaged by HanBio (Shanghai, China). When intervened, the cardiomyocytes and cardiac fibroblasts were infected by circSMAD3 overexpression adenovirus, circSMAD3 sh-RNA adenovirus and their control adenovirus with 10 MOI. *In vivo* experiment, circSMAD3 overexpression adeno-associated virus type 9 with cTnT or U6 promotor were packaged by HanBio (Shanghai, China), and injected to the C57BL/6J mice at a titer of  $5 \times 10^{12}$  v.g./mL (100 $\mu$ L per mouse) by tail vein before operation.

### Immunofluorescence analysis

Heart tissues were collected and fixed in 4% paraformaldehyde. Then tissue sections and culture cells were permeabilized with 0.5% Triton in PBS for 15 min and incubated in 5% Bovine Serum Albumin (BSA) for 1 h at room temperature following incubated at 4°C overnight with primary antibodies diluted in 5% BSA. The primary antibodies were used as follows: anti-cTnT antibody (1:200, Abcam, USA), anti-vimentin antibody (1:200, Abcam, USA), anti-CD31 antibody (1:200, Abcam, USA) and anti-YBX1 antibody (1:200, Abclonal, China). The samples were incubated with secondary antibodies (FITC mouse, CY3 rabbit, Servicebio, Wuhan, China) at 1:500 for 45 min, and washed three times with PBS. DAPI were incubated for another 15 min. The pictures were taken on a fluorescent microscope.

### Isolation of primary cardiomyocytes and cardiac fibroblasts

The isolation of cardiomyocytes (NMCM) and cardiac fibroblasts (MCF) were conducted from newborn mice. Briefly, neonatal hearts were taken out from newborn mice (0-3days), washed off the blood and cut into pieces at the ice. Then, the pieces were transferred to the 15mL tube with 7mL 1% collagenase type 2 and incubated at 37°C water bath for 7 min. The supernatant was removed into another 50mL tube with 1mL serum neutralizing. This digestion process was repeated seven times. After digestion, the supernatant was collected, filtrated through a cell strainer (200 meshes) and centrifuged at 4°C and 1000g for 8 min. The isolated cells were in the sediment and resuspended using DMEM with 10% fetal bovine serum to be seeded into plates and cultured. After 2 h, NMCMs were in the supernatant and MCF were adherent. The verification of cells was confirmed by immunoprecipitation analysis with cardiomyocyte special marker cTnT, fibroblasts special marker Vimentin, and endothelial cell marker CD31.

### Cell area measure

AC16 and NMCMs were seeded on a glass coverslip in 24-well dishes. After stimulation, the cells were washed by PBS buffer twice times, fixes in 4% paraformaldehyde and permeabilized with 0.5% Triton X-100 (Beyotime Bio, Shanghai, China) for 15 min respectively. Then, the sample were incubated with 0.1% phalloidine (Beyotime Bio, Shanghai, China) for 30 min at 37°C, following being incubated with DAPI at 1:1000 dilution for another 15 min coverslips were mounted on glass slides with mounting media. The pictures were taken using fluorescent microscopy. This process was replicated in a least three independent experiments.

### CCK8 assay

Cardiac fibroblasts were seeded into 96-well plates, and infected by circSMAD3 overexpression or shRNA adenovirus or transfected YBX1 overexpression vector and shRNA. The proliferation of cells was monitored at 72 h by CCK8 kit as manufacturer's instructions. The OD value was detected at 450 nm wave length.

### Wound healing assay

In brief, cardiac fibroblasts were seeded in 6-well plate with appropriate number. After the cells attached, the supernatant was discarded and the cells were washed using PBS buffer. 200 $\mu$ L tips were used to scratch and the floating cells were washed away by PBS buffer. The cells continued to be cultured by DMEM with serum free at 37°C. The pictures were taken by microscope, and the gap was calculated.

### 5-Ethynyl-2'-deoxyuridine (EdU) assay

The 5-ethynyl-2'-deoxyuridine (EdU) assay was conducted according to the Cell-Light EdU Apollo567 *In Vitro* Kit (RiboBio, Guangzhou, China). The cells were seeded into 48-well plates. After intervene, the cells were incubated with EdU solution at 1:1000 dilution at 37°C for 2 h, fixed by 4% paraformaldehyde and incubated with master buffer prepared as the protocol. DAPI was incubated for 15 min. The pictures were taken by fluorescence microscope.

### **Pull-down assay with biotinylated circSMAD3 probe**

The biotinylated probe was designed and synthesized by RiboBio (Guangzhou, China) specially binding to the junction area of circSMAD3, while the oligo probe was taken as a control. Approximately  $1 \times 10^7$  cells were harvested and lysed. The circSMAD3 probe was incubated with streptavidin magnetic beads (Life Technologies, USA) at room temperature for 1 h to generate probe-coated beads. The cell lysates were incubated with probe-coated beads at room temperature for 2 h. The complexes were washed two times and divided to two parts for RNA and protein extraction. The bound RNA in the pull-down materials were extracted using Trizol reagent and analyzed by qRT-PCR assay. The proteins in the complexes were detected by western blot. The sequence of probs is showed in [Table S5](#). The proteins identified in cardiomyocytes and cardiac fibroblasts were showed in [Tables S6](#) and [S7](#).

### **RNA immunoprecipitation (RIP)**

RIP was conducted using a Magna RIP Kit (Millipore, Billerica, MA, USA) following the manufacturer's instructions. Briefly, cells were washed by PBS buffer for two times and then lysed by IP lysis containing Rnase inhibitor and protease inhibitor. After centrifuging, the supernatant was retained for further treatment. The antibody was incubated with protein A/G beads for 1 h at room temperature. Then, the complexes of antibody and beads were incubated with cell supernatant overnight at 4°C. The RNA in complex was extracted by Trizol. The enrichment of circSMAD3, mSMAD3 and preSMAD3 was tested by qRT-PCR. The antibodies against YBX1 and IgG used for RIP were from Abclonal (Wuhan, China). The antibodies against DHX9 were from Santa Cruz company (USA).

### **Luciferase reporter assay**

The promotor sequence of ANP, BNP and MYH7 was inserted into the PGL3 luciferase reporter plasmid. The insertion was confirmed to be correct by sanger sequence. For the luciferase reporter assays, HEK293 cells were cultured in 24-well plates, and each well was transfected with 0.25 µg of reporter plasmid, YBX1 overexpressing vector and TK vector using Lipofectamine 2000 (Invitrogen, USA). After 48 h, the cells were lysed and the luciferase activities was detected according to the protocol of luciferase assay kit (Promega, Madison, WI, USA).

### **Chromatin immunoprecipitation (ChIP)**

The ChIP assay was performed using ChIP Kit (Beyotime Bio, Shanghai, China). In brief, Cardiomyocytes were seeded into 10 cm dishes. After treatment, the cells were fixed by formaldehyde at the final concentration of 1% for 10 min the cells were collected, lysed by IP lysis and treated by ultrasound to break the chromatin to pieces. These pieces were incubated with antibody overnight at 4°C. The DNA-antibody complexes were washed by wash buffer and incubated with protein A/G beads for 1 h at room temperature. and the DNA pieces were eluted by elution buffer and extracted by DNA purification Mini spin Kit (Beyotime Bio, Shanghai, China). The primers of ChIP were showed in [Table S2](#).

### **Transverse aortic constriction (TAC)**

All mice were C57Bl/6J male aged 7 weeks, purchased from Gempharmatech Co., Ltd (Jiangsu, China), and reared in Tongji medical college, Huazhong university of Science and Technology (Wuhan, China). In brief, when operated, the mice were anesthetized with xylazine (5 mg/kg) and ketamine (80 mg/kg) (Sigma, USA), cut the skin in front of the neck, and blunt dissection of the fascia, and cut the sternum to the second costal ridge angle. The aortic arch was caught by a smooth hook with a hole in its front end and constricted between the left and right carotid arteries using a 7-0 silk suture (Jinhuan, Shanghai, China). This protocols in our lab created a consistent peak pressure gradient of approximately 4000 across the constricted portion of the aorta detected by small animal ultrasound instrument.

### **Myocardial infraction (MI)**

The mice were injected with adeno-associated virus type 9 before undergoing MI. After 3 weeks, the mice were anesthetized with xylazine (5 mg/kg) and ketamine (80 mg/kg), and orotracheal intubation was performed. The hair was cut off on the left midaxillary and open the rib cage from the fourth rib, and blunt dissection of the fascia. The left anterior descending vessel was ligated with a 7-gauge thread (Jinhuan, Shanghai, China). Local pallor of the left anterior ventricular wall indicates successful surgery. Finally, the chest cavity was closed and sutured and the mice were observed in electric blanket to keep them warm and upregulate the survival rate.

### **Echocardiography**

After 8 weeks of TAC or 4 weeks of MI, the mice were detected for cardiac function by echocardiography. In brief, the mice were fixed in the supporting structure, and imaged using small animal ultrasound structure with B model or M model. Measurements were obtained from M-mode sampling and integrated EKV images taken in LV short axis at the mid-papillary level. The parameters of cardiac function undergoing TAC or MI are shown in [Tables S8](#) and [S9](#).

### **Data analysis**

The DHX9 CLIP-seq and FLASH sequencing data were downloaded from GEO database and the GSE number are GSM2258635, GSM2258636, GSM2363523, GSM2363519 and GSM2363521. The Fastq files were downloaded and then trimmed by Trim\_galore with default

parameters. The trimmed reads were mapped to the reference genomes (hg38) using bowtie2 (v2.2.0) with parameters `-very-sensitive -end-to-end -no-mixed -no-discordant -maxins = 200`. BigWig profiles was produced by Deeptools with default parameters and showed in Integrative Genomics Viewer (IGV).

### **QUANTIFICATION AND STATISTICAL ANALYSIS**

Statistical analysis was conducted using SPSS22.0 (IBM, SPSS, Chicago, IL, USA) or GraphPad7. Student's t-test, one way or two-way analysis of variance (ANOVA) was applied in multiple different groups experiments statistical analysis. All data are presented as the Mean  $\pm$  Standard deviation (SD) from three independent experiments unless otherwise noted. *p*-value <0.05 was considered statistically significant.